Diminished Ovarian Reserve Chemotherapy-Induced Mouse Model: A Tool for the Preclinical Assessment of New Therapies for Ovarian Damage

Anna Buigues, BSc[1,2], Maria Marchante, BSc[1,2], Sonia Herraiz, PhD[1,3,4], and Antonio Pellicer, MD[1,3,5]

Abstract

Diminished ovarian reserve (DOR) and primary ovarian insufficiency (POI) are primary factors leading to infertility. However, there is a lack of appropriate animal models of DOR usable for assessing new therapeutic strategies. In this study, we aimed to evaluate whether chemotherapy treatment in mice could reproduce features similar of that observed in women with DOR. Twenty-one Nonobese diabetic/severe combined immunodeficiency (NOD/SCID) female mice were allocated to 3 groups (n = 7/group): control, single dose of vehicle (Dimethyl Sulfoxide [DMSO]); DOR, single reduced chemotherapy dose; and POI, single standard chemotherapy dose. After 21 days, mice underwent ovarian hyperstimulation and mating. Part of the animals were harvested to analyze ovarian reserve, ovulation and fertilization rates, and morphology, apoptosis, and vascularization of the ovarian stroma. The remaining mice underwent multiple matings to assess pregnancy rates and litter sizes. The DOR and POI mice showed an impaired estrous cyclicity and a decrease in ovarian mass, number of follicles, Metaphase II (MII) oocytes, and embryos as well as in ovarian stroma vascularization. Mice in both models showed also an increase in the percentage of morphologically abnormal follicles, stromal degeneration, and apoptosis. Similar to that observed in DOR and POI patients, these impairments were less severe in DOR than in POI mice. None of the POI females were able to achieve a pregnancy. Meanwhile, DOR females achieved several consecutive pregnancies, although litter size was decreased when compared to controls. In conclusion, a mouse model which displayed most of the ovarian characteristics and fertility outcomes of women with DOR has been established using a single dose of chemotherapy.

Introduction

Female infertility has increased in the recent decades. The primary factors leading to infertility are due to delayed childbearing, which is associated with reproductive aging and diminished ovarian reserve (DOR).[1] Although research efforts into infertility have increased, identifying the physiological and molecular underpinnings of DOR remains challenging in humans. Further, there is a lack of appropriate, affordable, and reproducible animal models in which to assess new therapeutic strategies to increased their fertility.

A DOR associates with poor fertility outcomes and occurs as women get older, since their ovarian reserve naturally declines with age.[2] A DOR is distinct from primary ovarian insufficiency (POI), in which patients show amenorrhea and a complete loss of ovarian function before the age of 40 years. The POI represents the worse-case ovarian condition.[3] Nevertheless, even when ovaries lose their ability to ovulate, it remains a pool of dormant residual follicles that could be rescue to growth.[4-6]

There are several reports of mouse gene knockout models with accelerated reproductive aging and phenotypes comparable to POI in humans.[7] These include the follitropin receptor knockout (FORKO) mouse,[8] the dioxin/aryl hydrocarbon receptor (AhR) knockout model,[9,10] and the Glutamate-cysteine ligase modifier subunit null mice.[11] The FORKO female mice have a chronic depletion of estrogen and ovarian failure at an early

[1] IVI Foundation, Valencia Spain
[2] Department of Pediatrics, Obstetrics and Gynecology, School of Medicine, Valencia University, Valencia, Spain
[3] Reproductive Medicine Research Group, IIS La Fe, Valencia, Spain
[4] IVI-RMA Valencia, Valencia, Spain
[5] IVI-RMA Rome, Rome, Italy

Corresponding Author:
Sonia Herraiz, IVI Foundation, Valencia, Spain. Av. Fernando Abril Martorell, 106-TorreA-Planta1. 46026 Valencia, Spain.
Email: sonia.herraiz@ivirma.com

developmental stage, with a 45% reduction in ovarian size due to a decrease in growing follicles.[8] The AhR null females have a small litter size and, at birth, aberrant follicular development (54% fewer astral follicles compared to wild-type females) induced by inadequate hormone levels early in life. These knockout models have several limitations; in particular, the ovaries in these models are affected at early developmental stages and normal reproductive systems never form. The reproductive function of POI and DOR women is normal when patients are young, and the ovarian aging phenotype, although accelerated, appears later in life. Therefore, these existing mouse models do not recapitulate the human phenotype. Additionally, these models can exhibit uterine alterations. The $Gclm^{-/-}$ knockout model does not display these limitations, showed similar numbers of follicles to that of $Gclm^{+/+}$ mice, and exhibited an accelerated decline with age and altered oocyte quality.[11] However, all knockout models are expensive and difficult to obtain and require continuous genotyping of the offspring.

With these limitations in mind, we propose to take advantage of the associated gonadotoxicity of chemotherapeutic drugs to develop animal models of ovarian damage. Treatment with high-dose chemotherapy in women may negatively affect the ovary. Clinically, the effect of cytotoxic treatments on the ovary can range from partial damage that reduces fertility to complete destruction of the follicular pool and tissue atrophy, leading to POI and a loss of fertility.[12] The degree of gonadotoxicity varies for the different groups of chemotherapeutic drugs. Women treated with the alkylating agents cyclophosphamide (Cy), chlorambucil, melphalan, busulfan (Bu), nitrogen mustard, and procarabazin have the highest risk of ovarian failure, while platinum-based compounds such as cisplatin cause a medium risk for POI.[13]

Some mouse models of chemotherapy-induced POI have been partially established,[14] but to date, no animal model for the less severe DOR condition has been reported. In the present study, we aimed to develop a mouse model of DOR by administering chemotherapy and to thoroughly characterize the broad spectrum of ovarian effects seen in the POI model. In order that these established models could be used to test therapeutic strategies from human origin without adverse immune consequences, an inmunodeficient strain (NOD/SCID) was used.

Materials and Methods

Ethics Statement

All animal experiments were approved by the institutional review board and the Ethics Committee (A1484581669445) from University of Valencia, Valencia, Spain.

Study Design

The POI and DOR conditions were induced in mice by a standard and reduced chemotherapy (ChT) regimens, respectively. Total body masses and estrous cycles were monitored daily for 21 days after ChT administration. Then, mice underwent ovarian hyperstimulation and mating with fertile males. Four mice of each group were euthanized after mating to recover ovaries and to collect Metaphase II (MII) oocytes and embryos from the oviduct. The remaining mice were allowed to deliver and then were paired with fertile males during the next 3 months to enable mating.

Animal Models

Twenty-one, 8-week-old female Nonobese diabetic/severe combined immunodeficiency (NOD-SCID) mice (Charles River Laboratories, Saint-Germain-Nuelles, France) were randomly allocated to the following experimental groups(n = 7/group): Control (vehicle), DOR, or POI. Mice in the DOR group were treated with a reduced ChT regimen consisting of a single intraperitoneal (IP) injection of 1.2 mg/kg Bu and 12 mg/kg Cy (Sigma, St Louis, Michigan), resuspended in Dimethyl Sulfoxide (DMSO). Meanwhile, mice in the POI group were treated with a standard regimen[15,16] consisting of a single IP dose of 12 mg/kg Bu and 120 mg/kg Cy. Control mice received an IP injection of DMSO (vehicle).

On day 21 after ChT administration, mice underwent ovarian hyperstimulation with 10 Interational Units (IU) of pregnant mare serum gonadotropin (PMSG; Sigma) followed by 10 IU of human chorionic gonadotropin (hCG) 48 hours later and then mated with fertile males. Four mice of each group were euthanized by cervical dislocation 48 hours after hCG injection to recover ovulated oocytes and 2-cell embryos from the oviduct. Ovaries were also collected, weighed, and immediately fixed in neutral-buffered formalin to analyze ovarian reserve, follicular development, vascularization, apoptosis, and cell density. The remaining animals (n = 3/group) were allowed to deliver after mating. After the first offspring, females underwent 3 mating attempts by pairing with fertile males for 12 weeks. The number of pregnancies, litter size, sex distribution, and mass of the offspring were monitored for all females in each attempt. During the entire experiment, all the mice were fed a standard diet ad libitum and housed in the specific pathogen-free zone in a 12:12-hour light–dark cycle. Survival, behavioral, and body mass data were recorded daily to assess overall health disparities between the groups. For the survival rate analysis, data were obtained from a subset of 15 animals/group included in a side experiment in order to properly evaluate any significant effect on animal health and mortality and to increase the statistical power of the Kaplan-Meier test.

Estrous Cycle Determination

Vaginal smears were taken daily (between 10 AM and 11 AM) throughout 21 days after treatment, using a normal saline solution, pipette tips, and a pipette teat. In order to avoid pseudo-estrous cyclicity, the pipette tip was not introduced into the vagina orifice. Dried smears were stained with 1% Crystal Violet (Sigma-Aldrich, St. Louis, MO, USA) for 1 minute, rinsed twice with distilled water, and dried at room temperature. The slides were then examined by 2 observers under a

light microscope, and the stage of the cycle was determined as follows: proestrous (mainly epithelial cells in the smear), estrous (mainly cornified cells in the smear), and diestrous (leukocytes in fair abundance in the smear). The estrous cycle length was determined as described previously.[17]

Follicular Counts

Ovaries were fixed in formalin, embedded in paraffin, and cut into 4-μm thick sections. Every fifth section was stained with hematoxylin–eosin (H&E) to perform follicular counts. To avoid double counting, normal follicles were only counted when the oocyte nucleus was present in the section and were classified as described previously.[18] Follicles were considered morphologically abnormal when degeneration and necrosis of granulosa cells and/or oocytes were observed. All H&E sections were examined by 2 observers (A.B. and M.M.).

Analysis of MII Oocytes and 2-Cell Embryos

Oviducts were harvested and cut between the ovary and the uterus. Oviducts were then placed in FHM medium (Vitrolife, Göteborg, Sweden) in a small Petri dish. The embryos and oocytes from the oviduct were expelled by inserting a 30-gauge needle into the infundibulum and passing FHM medium through the oviduct. The obtained oocytes and embryos were isolated and classified using a binocular loupe.

Evaluation of Ovarian Stroma and Apoptosis

The effects of ChT on the structure, vascularization, and apoptosis of the ovarian stroma and follicles were evaluated. Degeneration of the ovarian stroma was studied in H&E-stained sections using high-magnification images (20×) of each sample obtained with a bright-field microscope. The areas within the ovaries, where tissue structure was lost and nuclei were absent, were considered degenerate. The degenerate area with respect to total area were quantified using Image Pro-plus software.

To assess vascularization, double immunofluorescence with isolectin B4, specifically labeling endothelial cells, and α-smooth muscle actin, to stain mature vessels, was used as described previously.[19] Four random ovarian sections per sample were assayed. High-magnification images (20×) were obtained using a bright-field microscope with a fluorescence module and a digital camera (LEICA DM4000B and DFC450C; Leica Microsystems GmbH, Germany) and then analyzed using the Image Pro-plus software (Media Cybernetics, Carlsbad, California). Lectin-positive areas were considered vessels, and microvessel density was determined as lectin-positive area by total area.

Finally, apoptosis was assessed by the TdT (terminal deoxyribonucleotidyl transferase)-mediated dUTP nick-end labeling (TUNEL) assay using the TMR red in situ cell death detection kit (Roche Diagnostics, Risch-Rotkreuz, Sweden) as described previously for ovarian tissue.[20] To quantify apoptotic cells, the percentage of TUNEL-positive cells was assessed in 4 sections per sample. High-magnification images were obtained and analyzed by Image Pro-Plus as described earlier.

Statistics

All data are presented as the mean (SD). The Kruskall-Wallis test was used to compare results between groups, and 2-by-2 comparisons were performed by the Mann-Whitney U test. Kaplan-Meier analysis was used to compare survival between the groups. Values of $P < .05$ were considered statistically significant. All analyses were performed using SPSS 22.0 (IBM, Somers, New York).

Results

Body and Ovarian Mass

Immediately after ChT administration, mice in the DOR and POI groups exhibited side effects: piloerection, a hunched posture, and reduced activity. For DOI mice, these effects only occurred immediately after the injection, while the POI mice exhibited more extreme and longer lasting (2-3 days) symptoms. One hundred percent of mice in the reduced ChT (DOR) group survived (15 of 15), but only 80% of the POI mice lived (12 of 15) until the end of the experimental period (Figure 1A) for all animals included in the survival and health evaluation experiments.

In the necropsy, macroscopic alternations or differences were not observed between DOR/POI and control animals. We detected a significant percentage of reduction in body mass on day 1 following injection in both models (control: 0.5 [0.7%], DOR model: −5.1 [3.3%], POI model: −13.8 [1.7%]; $P = .04$ and $P = .021$, respectively). Body mass loss was lower and quickly recovered in the DOR mice (Figure 1B).

At the time of ovarian stimulation and ovarian/oviducts collection, DOR and POI females did not show clinical signs of major side effects, as no differences were detected for body mass (Figure 1B), general health, and behavioral status. Moreover, in the necropsy, macroscopic alternations or differences were not observed between DOR/POI and control animals.

In both models, ChT reduced ovarian size (Figure 1C), with this decrease being significantly ($P = .021$) less severe in DOR mice than in POI mice, which had a 5-fold reduction in ovarian mass when compared to controls (control: 45.7 [2.0] mg, DOR model: 18.8 [2.3] mg, POI model: 9.0 [3.8] mg). The ovarian–body mass ratio was assessed to rule out body mass influence, and the same pattern was observed (Figure 1D).

Estrous Cycle

In the DOR model, the estrous cycle was 2-fold longer than that of the controls (control: 5.9 [0.8] days, DOR: 11.7 [1.9] days; $P = .046$) until cessation occurred 12.3 [0.5] days after treatment. In the POI model, cycling stopped earlier (8.3 [0.5]; $P = .04$), and the cycles remained arrested in the diestrous phase (Figure 2A).
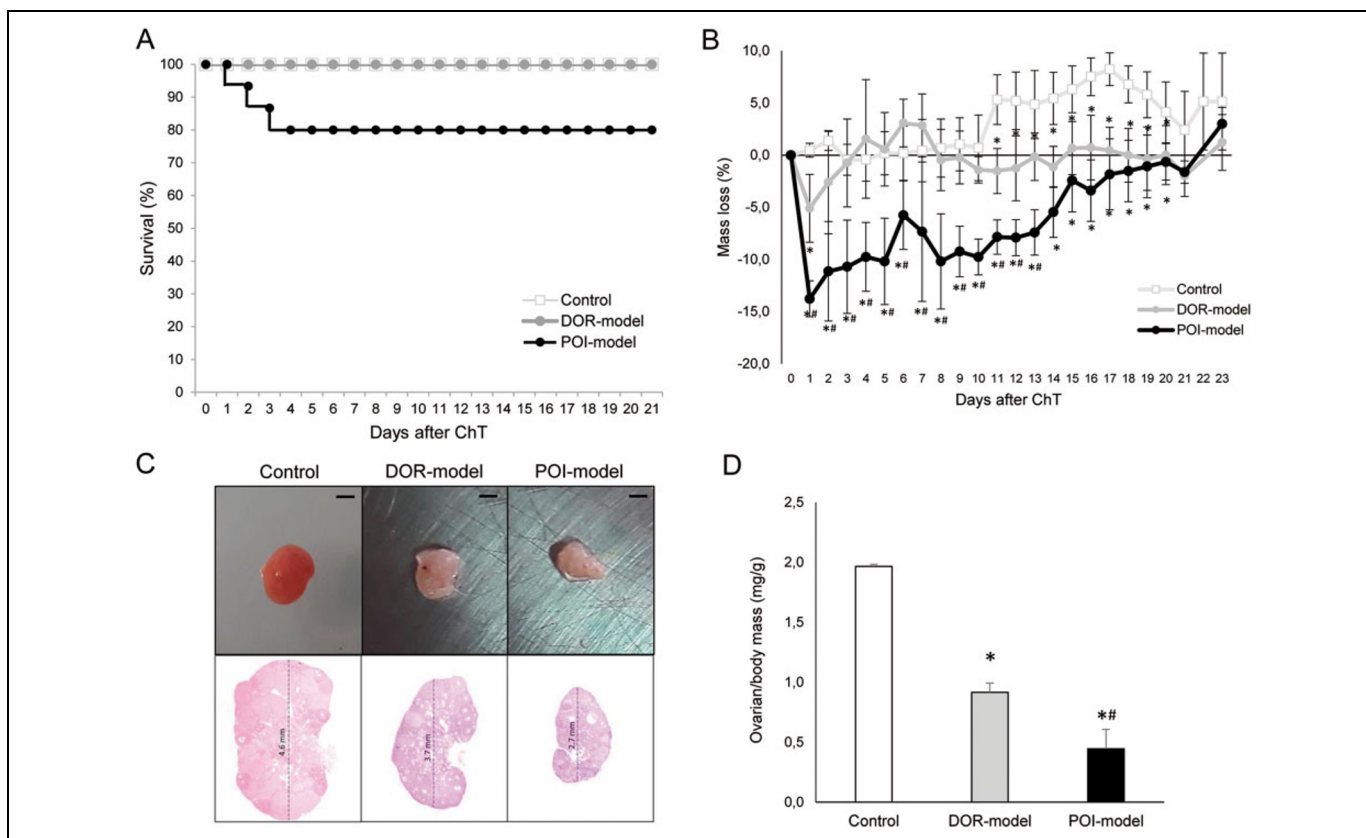
Figure 1. Effects on survival and body and ovarian mass. A, Kaplan-Meier survival curves for all experimental groups (n = 15/group). No mice in the control and diminished ovarian reserve (DOR) groups died, while 20% of mice in the primary ovarian insufficiency (POI) group (3 of 15) died. However, no statistically significant differences were detected. B, Body mass follow-up (n = 4/group). The chemotherapy (ChT) treatment induced a significant decrease in body mass in both the DOR and POI model. The loss was significantly higher (3-fold) in POI than DOR mice. C, Ovarian macroscopic images and hematoxylin-eosin (H&E)-stained middle ovarian sections (established considering the total number of sections from each ovary) from all experimental groups. Black scale bars = 1 mm. D, Ovarian mass normalized to total body mass (n = 4/group). Ovarian size and mass decreased in a dose-dependent manner with ChT administration. Kaplan-Meier analysis (in A) and Mann-Whitney U test (in B and D) were used to compare results between groups. Values of $P < .05$ were considered statistically significant. $*P < .05$ compared with control group. $^{#}P < .05$ when compared to the DOR group.

Over 21 days of monitoring following treatment, control mice completed a total of 4 (1) cycles. In both the DOR and POI models, the number of cycles was reduced ($P = .026$ and $P = .029$, respectively), and the number of consecutive days in diestrous increased ($P = .031$ and $P = .032$, respectively; Figure 2B and C), with the time spent in diestrous being over 59.5 (11.9%) of the follow-up period in the POI mice (Figure 2D).

Ovarian Reserve and Follicular Development

The total number of follicles was significantly reduced in DOR and POI models when compared to controls ($P = .034$ in both cases) as shown in Figure 3A. Follicular depletion was higher in the POI than in the DOR ovaries (83% vs 33%; $P = .021$). Primordial follicles were the most affected population in both models (55% depletion in DOR and 97% in POI), while growing follicles were less affected (29% depletion in DOR and 70% in POI) as shown in Figure 3B. The growing–dormant follicle ratio was dose dependently increased (control: 5.6 [1.2], DOR: 8.9 [1.5], POI: 97.0 [44.6]; $P = .034$).

When both models were compared, we found that primordial follicles were almost absent in the POI but not in the DOR ovaries (DOR = 88.0 [27.4] vs POI = 0.75 [1.5]; $P = .018$). Statistically significant differences were also observed in primary (DOR = 491.0 [84.7], POI = 183.5 [159.0]; $P = .020$), secondary (DOR = 154.8 [72.0], POI = 6.3 [1.7]; $P = .021$), tertiary (DOR = 52.8 [8.7], POI = 11.8 [4.7]; $P = .020$), and antral (DOR = 45.8 [9.4], POI = 16.0 [10.6]; $P = .020$) follicles (Figure 3B).

Morphologically abnormal follicles, mainly found in the antral population, were detected in ovaries from 3 groups but increased in both models compared to controls (control: 0.83 [0.42%], DOR: 10.92 [0.99%], POI: 21.98 [3.89%]; $P = .049$ and $P = .034$, respectively; Figure 3C and D).

Fertility Outcomes

Both chemotherapeutic treatments decreased the number of MII oocytes and 2-cell embryos (Figure 3E-G). When both
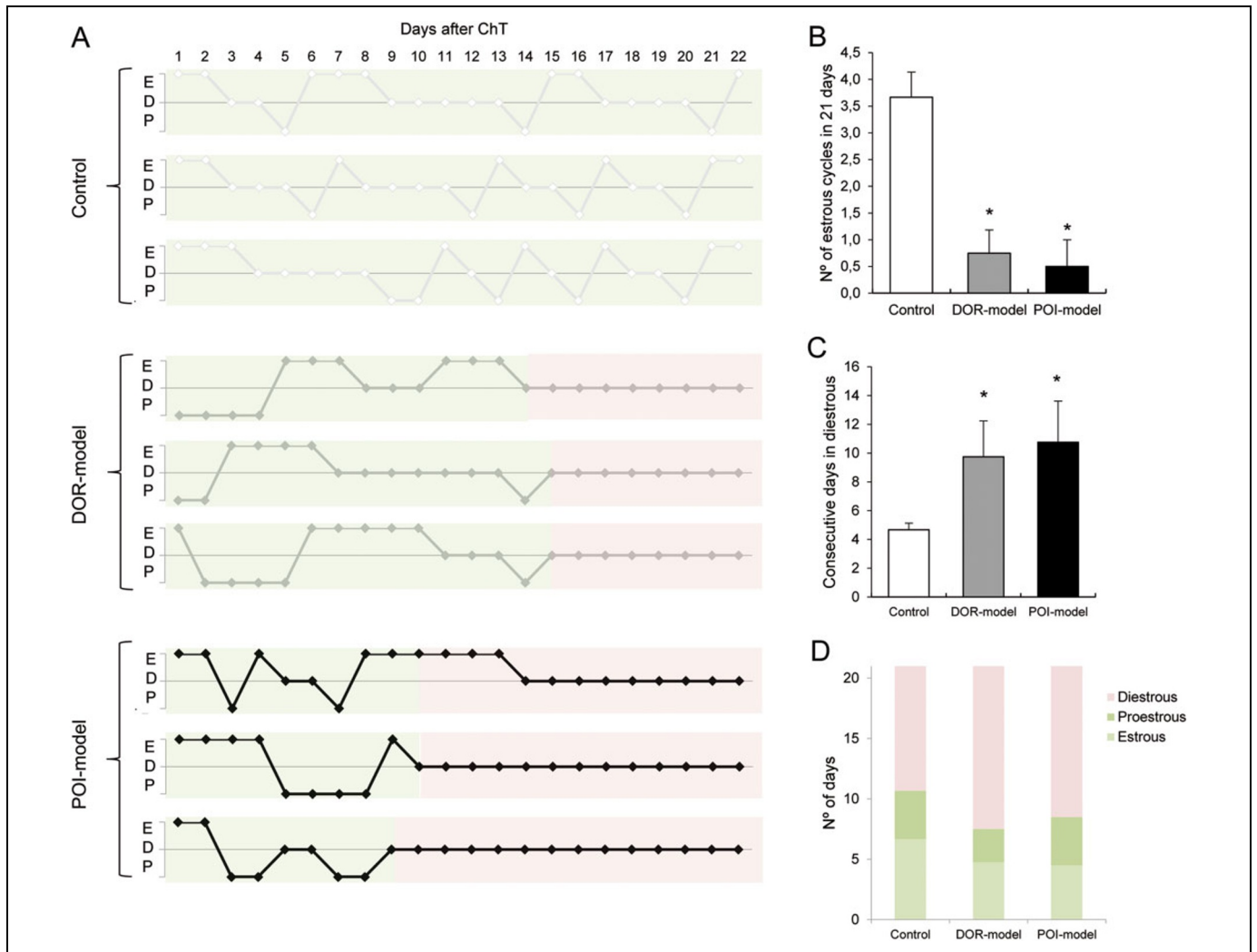
Figure 2. Estrous cycle follow-up. A, Estrous cycles were monitored for 21 days. Periods with regular cyclicity are green shaded while nonregular ones are red shaded. Control mice showed regular cyclicity, while mice from both chemotherapy-treated models had impaired cyclicity, with this occurring later in diminished ovarian reserve (DOR) compared to primary ovarian insufficiency (POI) mice. E, Estrous; D, Diestrous; P, Proestrous. B, Number of estrous cycles completed in 21 days. The number of estrous cycles was significantly reduced in DOR and POI mice. C, Consecutive days in diestrous phase increased in DOR and POI models compared to controls. D, Number of days in each phase. When compared to the control group, DOR and POI groups spent more time in the diestrous leukocyte-enriched phase. Mann-Whitney U test was used to compare results between groups. Values of $P < .05$ were considered statistically significant. *$P < .05$ compared with control group. n = 4/group.

models were compared (n = 4/each group), there was no difference in the total number of MII oocytes, but viable MIIs (DOR: 6.3 [2.0], POI: 1.7 [0.6]), the fertilization rate, and the number of 2-cell embryos ($P = .046$ and $P = .034$, respectively) were lower in the POI model than in the DOR model.

None of the POI females was able to achieve a pregnancy after several attempts. Meanwhile, in the DOR model, females achieved several consecutive pregnancies and delivered healthy pups, although the litter size decreased (Table 1). The ChT did not affect sex distribution and pups' mass (control: 1.6 [0.1], DOR model: 1.5 [01]; $P = $ Not Statistically Significant (NS)).

Effects on Ovarian Stroma and Apoptosis

Ovarian structure was disrupted in the middle stromal region after ChT, especially in the POI model. The main features of the DOR ovaries were fibrosis and the presence of large stromal holes, while POI was characterized by many small holes (Figure 4A). Stromal degeneration was increased 2.5 times and 3.3 times in the DOR and the POI models, respectively ($P = .049$ and $P = .034$). However, no statistically significant differences were detected when both models were compared (DOR: 11.71 [4.18%], POI: 15.62 [5.39%]; $P = $ NS).

A dose-dependent decrease in microvessel density was also detected after ChT administration as shown in Figure 4B (control: 4.7 [1.0], DOR: 2.7 [0.9], POI: 1.8 [0.7%]; $P < .05$).
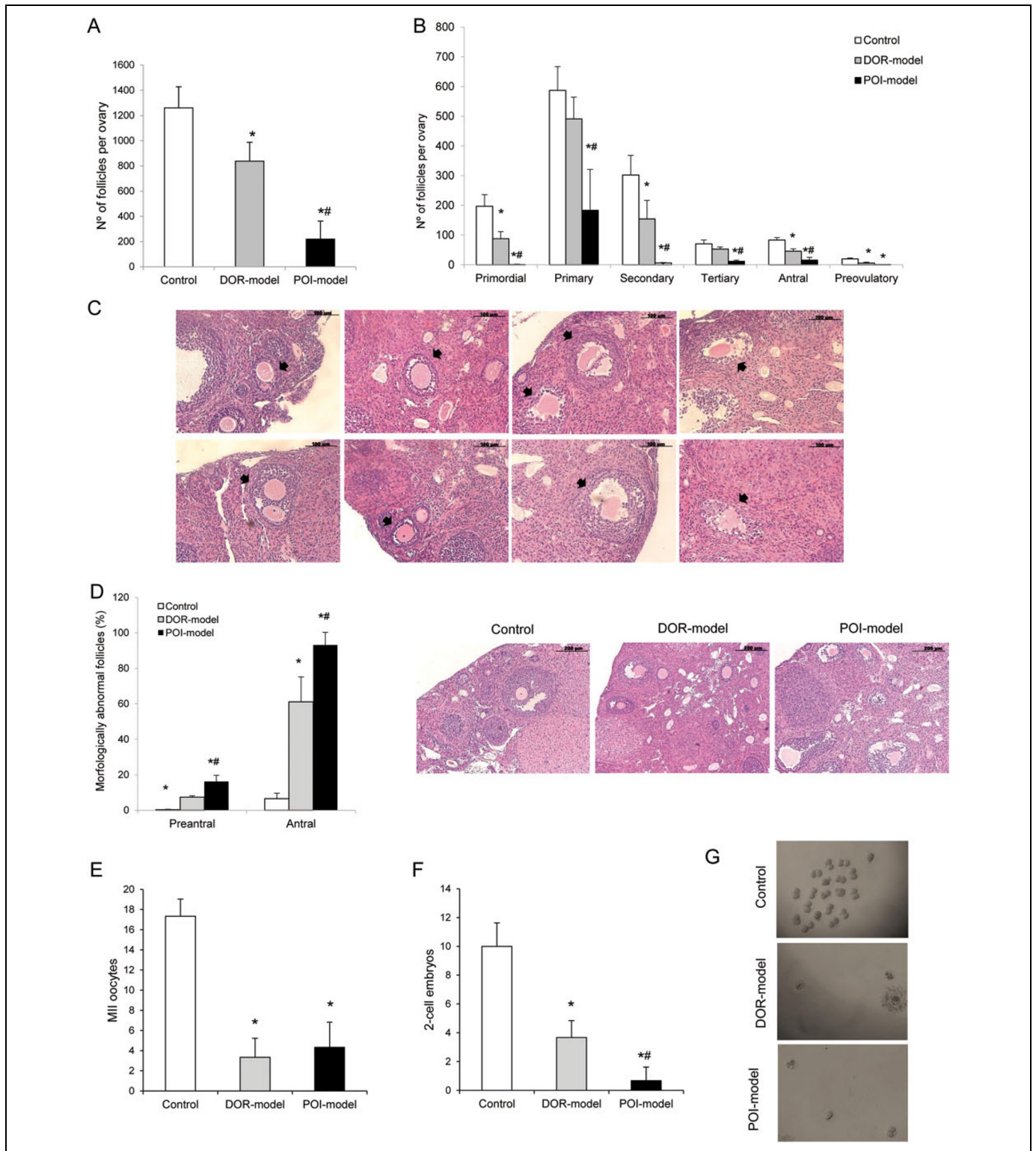
Figure 3. Effects on ovarian reserve, MII, and embryos. A, Number of total follicles in each group (n = 4/group). Total follicle numbers were decreased by chemotherapy, with this depletion being higher in primary ovarian insufficiency (POI) than diminished ovarian reserve (DOR) mice. B, Number of primordial, primary, secondary, tertiary, antral, and preovulatory follicles in control, DOR and POI mice (n = 4/group). All follicular populations decreased in DOR mice but, more dramatically in POI mice. C, Hematoxylin and eosin stained sections showing morphologically abnormal follicles (arrows) found in ovarian sections, especially in DOR and POI models. From left to right, double oocyte follicles, vacuolated preantral follicles with abnormal granulosa, antral follicles with abnormal granulosa and/or disrupted organization of the basal lamina, and degenerated follicles were observed. Black scale bar = 100 μm. D, Percentage of morphologically abnormal preantral and antral

Table 1. Fertility Outcomes During 12 Weeks.[a]

Outcome	Control, n = 3	DOR Model, n = 3	POI Model, n = 3
Percentage of pregnancy			
1st mating	100%	33%	0%
2nd mating	100%	66%	0%
3rd mating	100%	33%	0%
Total	100 (0%)	44 (15%)	0 (0%)[b,c]
Litter size (n)			
1st mating	10 (1)	7 (0)	0 (0)
2nd mating	9 (1)	6 (1)	0 (0)
3rd mating	10 (1)	5 (0)	0 (0)
Total	10 (1)	6 (0)[b]	0 (0)[b,c]

Abbreviations: DOR, diminished ovarian reserve; POI, primary ovarian insufficiency; SD, standard deviation.
[a]Values are shown as the mean (SD) for percentage of pregnancy and litter size.
[b]$P < .05$ compared with the control group.
[c]$P < .05$ when compared to the DOR model.

A few apoptotic cells were detected within control ovaries, mainly in the granulosa layers of antral follicles. Meanwhile, several follicles with many apoptotic granulosa cells were detected in ChT-treated ovaries (Figure 4C). The pre cells and the oocytes of primordial follicles lacked TUNEL staining in all analyzed samples. A 40-fold increase in the percentage of total apoptotic cells was detected in both DOR and POI ovaries (control: 0.01 [0.01%], DOR model: 0.52 [0.33%], POI model: 0.52 [0.33%]).

Discussion

A chemotherapy-induced DOR model has been established in this study. Specifically, by using a reduced chemotherapeutic regimen, we achieved less severe ovarian damage and a moderated reduction in body mass, ovarian reserve, number of viable MII oocytes, embryos, litter size, and intraovarian vascularization. Additionally, we characterized the full spectrum of reproductive effects in a previously described POI model.

Administration of various chemotherapeutic drugs have been used to deplete ovarian follicles and to POI mouse models,[14] with the alkylating drugs Cy and Bu being the most commonly used.[21,22] This approach represents a reproducible, easier, faster to develop, and less costly method than knockout models. Cy and Bu are frequently employed for treatment of breast cancer and hematological malignancies such as leukemia and lymphomas, which are the cancers that most affect women's fertility.[13,23] Due to this fact, having an established

models of DOR and POI induced by these agents would be of great value for investigation and translational medicine.

In addition to chemotherapeutic drugs, other chemicals as 4-vinylcyclohexene diepoxide (VCD), with selective toxicity on primordial and primary follicles, have been used to established models of POI.[24-26] Its administration does not have systemic toxicity and represents an easy, fast, and low costly approach to develop models of POI. However, mice of the VCD-induced POI model show a complete depletion in primordial follicles, which is not consistent with that observed in POI patients.[5,6] Moreover, low doses of VCD generate this effect,[26] so it would be difficult to use with the purpose to mimic a DOR condition. In this study, a combination of Cy and Bu was tested at 2 different dosages to achieve different degrees of ovarian damage. Due to the relevance and increasing incidence of DOR,[27] a reduced dose was used to establish a less severe ovarian condition. Our model was based on the idea that chemotherapy-induced follicular loss is produced in a dose-dependent manner, as reported in other animal studies.[28,29] The highest dose, equivalent to that used in oncologic patients[30,31] and consisting in a single dose of 120 mg/kg of Cy and 12 mg/kg of Bu, has been used to induce follicle depletion in several animal studies of POI.[15,16] However, its effects on ovarian tissues had not been fully characterized.

The absence of mortality observed in our DOR model highlights the lower cytotoxicity of this reduced dosage, which is also supported by a 2-fold lower body mass reduction when compared to the mass reduction in POI mice. We observed increased mortality in the POI model during the first 3 days after chemotherapy, but this difference was not statistically significant, in agreement with previous reports.[32] In fact, this dose has been described as the highest dose to achieve irreversible infertility[33] while allowing animal survival. At the time of ovarian stimulation and ovarian/oviducts collection, neither DOR nor POI females showed chemotherapy systemic effects as indicated by clinical signs, weight loss, and mortality data. Therefore, it is unlikely that observed effects on fertility outcomes were the result of systemic toxicity in addition to ovarian toxicity.

The estrous cycle is considered one of the most easily measurable markers of reproductive decline. In fact, its length and cytology stage reflect the hormonal milieu that maintains ovarian function.[34] Diminished ovarian reserve mice displayed an elongation in the phases of the estrous cycle, one of the first symptoms of ovarian aging[34] after chemotherapy. In POI mice, the estrous cycle arrested in diestrous, which might reflect insufficient E_2 secretion due to a reduced number of mature follicles. This impairment was detected shortly after ChT, consistent with a rapid fertility loss after this highly gonadotoxic

Figure 3. (Continued). follicles (left panel, n = 4/group) and representative images of morphologically abnormal follicles (right panel, black scale bar = 200 μm). Both percentages increased with chemotherapy. However, this increase was lower in DOR compared to POI mice. E, The number of MII oocytes and (F) Two-cell embryos recovered from the oviduct after an ovarian hyperstimulation were lower in both POI and DOR models when compared to controls (n = 4/group). G, Representative images of MII oocytes and embryos. Mann-Whitney *U* test was used to compare results between groups. Values of $P < .05$ were considered statistically significant. *$P < .05$ compared with control group. #$P < .05$ when compared to DOR model.
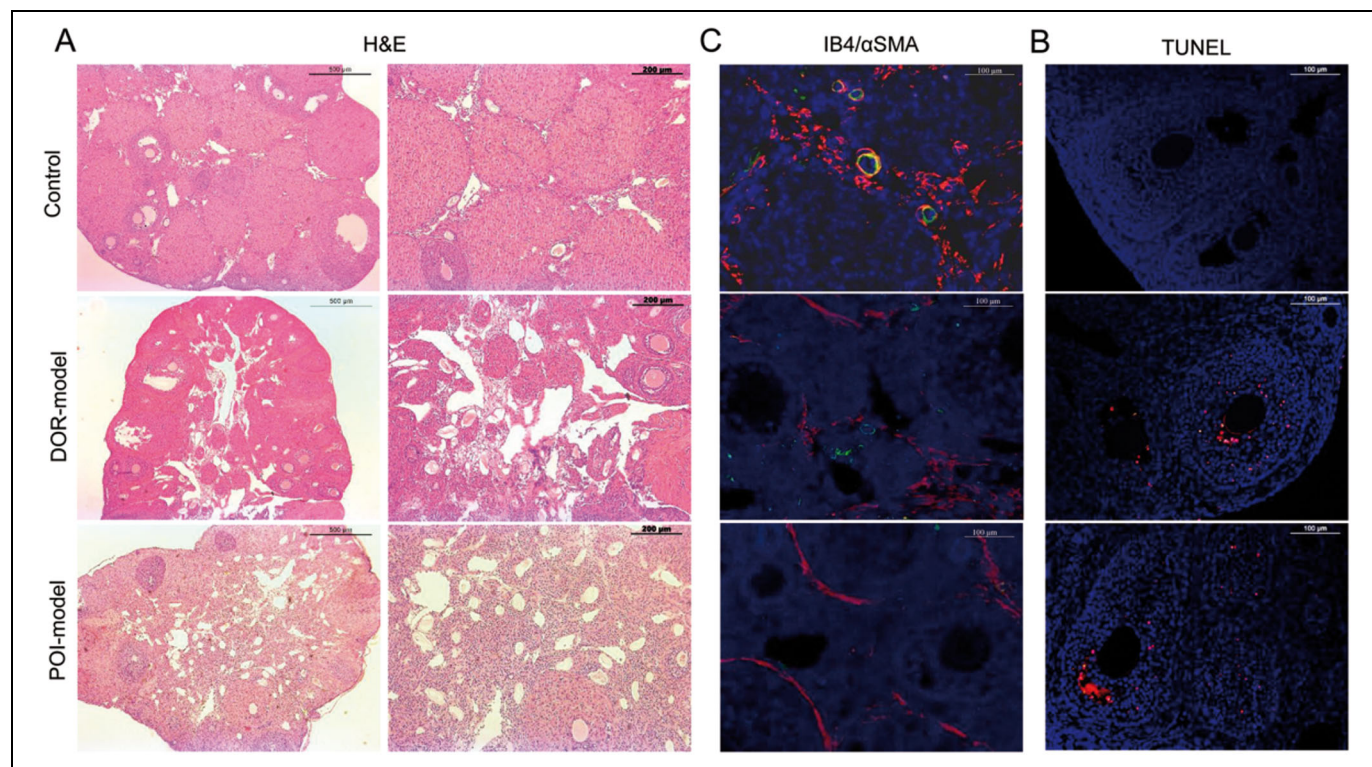
Figure 4. Ovarian stroma, apoptosis, and vascularization analyses. A, Hematoxylin and eosin (H&E) stained sections showing stromal degeneration and fibrosis in treated ovaries at 5× (left panels) and 10× (right panels) magnification (n = 4/group). B, Vascularization assay showing isolectin B4 (IB4) in green and α-smooth muscle actin (α-SMA) in red. Green signal represents new vessels, green signal surrounded by red signal represents mature vessels, and red signal alone corresponds to stromal cells surrounding the follicles. Nuclei were stained in blue with DAPI. Vascularization within ovaries was significantly reduced in diminished ovarian reserve (DOR) and primary ovarian insufficiency (POI) samples (n = 4/group). C, TdT (terminal deoxyribonucleotidyl transferase)-mediated dUTP nick-end labeling (TUNEL) staining showing apoptotic cells (red) and cell nuclei (blue, DAPI). Apoptosis was higher in the DOR and POI models compared to controls (n = 4/group). Black scale bar in A left panels = 500 μm, black scale bar in A right panels = 200 μm and white scale bar = 100 μm.

treatment.[35] Despite the estrous cycle imbalance, DOR and POI females were able to ovulate a reduced number of MII oocytes into the oviducts, suggesting that residual FSH-stimulable follicles were still able to respond after the injection of PMSG and hCG. This result suggests that estrous cycle dysregulation might be a consequence of a reduced number but not a total depletion of mature follicles.

As in patients with POI,[36,37] our POI mice showed small-sized ovaries, reflecting follicular depletion induced by Bu/Cy,[38] while DOR mice exhibited a lesser reduction in ovarian size.

Ovarian hyperstimulation and harvesting of ovaries at the time point of 21 days, period necessary from primordial to ovulatory follicle in mice,[39]allowed the assessment of short-term effects. Animals from the control group showed reduced number of primordial follicles. This finding might be explained by the difficulty of distinguishing early growing follicles (primary) from resting follicles in mice based on morphology and size.[39-41] In fact, when both populations were considered together as a continuous group,[42] the balance between the primordial/primary and the growing population was restored.

Decreased follicular numbers were detected in both ovarian conditions, especially for the dormant primordial population,

as previously reported for Cy treatments.[12] Additionally, a reduced number of antral follicles and MII oocytes was also observed in the DOR mice as described for DOR patients.[2] Interestingly, we found that the total number of MII in the DOR model was similar to that observed in the POI model, where the antral population was significantly reduced. This finding could be explained by a higher percentage of morphologically abnormal antral follicles in POI mice. Abnormal antral follicles affected by chemotherapy are able to achieve the preovulatory stage and be ovulated leading to poor-quality oocytes.[14] This finding could explain the higher number of viable MII oocytes and 2-cell embryos in our DOR model compared to the POI model. Consistent with the infertile phenotype of patients with cancer undergoing chemotherapy, females in the POI model were unable to become pregnant even in the first mating attempt. Meanwhile, DOR females achieved several pregnancies and delivered healthy pups, although the pregnancy rate and litter size were reduced when compared to those of the controls. All together, these findings evidenced consistent reproductive phenotypes for both conditions, as similar characteristics were observed in a recent work from our group.[19]

The status of the ovarian stroma was also assessed in both models due to their impaired condition in patients with DOR

and POI. In fact, ovarian aging is associated with the differentiation of functional ovarian tissue in fibrotic tissue.[43] Furthermore, diminished ovarian vascularization has been associated with impaired ovarian function in women[44] and contributes to poor ovarian response[45,46] due to reduced delivery of gonadotropic hormones and growth factors involved in folliculogenesis.[47,48] The DOR and POI models established in this study displayed stromal degeneration and decreased ovarian vascularization, which were milder in the DOR mice. Therefore, these models recapitulate characteristics of the ovarian stroma observed in patients with these ovarian conditions.

When apoptosis was analyzed in ovarian samples, apoptotic cells were mainly detected in granulosa cells as previously reported[12] perhaps due to their high mitotic index.[49,50] Interestingly, although direct toxicity on primordial follicles has also been described as a direct effect of chemotherapy,[51] we did not detect apoptosis in primordial follicles. This finding and the fact that DOR females were able to get pregnant 3 months after chemotherapy suggests that in DOR model it remains a pool of healthy primordial follicles, which can be recruited, growth to mature state, be ovulated, and fertilized. In fact, the remaining follicles in chemotherapy-induced models are not completely impaired, as the treatment of these females with bone marrow stem cell increased the number of viable MII oocytes, embryos, and healthy pups/litter.[19] Furthermore, a dose-dependent decrease in primordial populations was observed and could be attributed to the burnout effect and to a lack of suppression mechanisms induced by growing follicles on the follicular activation process.[12] No differences were detected in apoptosis, perhaps due to a reduction in the cytotoxic effects of Cy and Bu over the time.[14]

In summary, in this study, inexpensive and reproducible mouse models of DOR and POI were established by using a single dose of chemotherapy. Because they are chemotherapy-induced DOR and POI situations, they may not be generalizable to other causes. However, these mouse models displayed most of the ovarian characteristics and fertility outcomes observed in women with DOR and POI regardless of they cause. Furthermore, by using an immunodeficient, strain these models may be reliable tools to test therapeutic strategies, from human origin (eg, adult stem cells, plasmas, etc)[19,52] without adverse immune consequences, for the increasing numbers of patients with these conditions.

Authors' Note

A.B. conducted experimental studies, analyzed data, and wrote the manuscript. S.H. designed and conducted experiments, analyzed data, and wrote the manuscript. M.M. contributed to conducting animal experiments. A.P. designed, supervised, and coordinated the study, analyzed data, and critically revised the manuscript.

Declaration of Conflicting Interests

The author(s) declared no potential conflicts of interest with respect to the research, authorship, and/or publication of this article.

References

1. Munne S, Cohen J, Sable D. Preimplantation genetic diagnosis for advanced maternal age and other indications. *Fertil Steril*. 2002; 78(2):234-236.

2. Cohen J, Chabbert-Buffet N, Darai E. Diminished ovarian reserve, premature ovarian failure, poor ovarian responde—a plea for universal definitions. *J Assist Reprod Genet*. 2015;32(12): 1709-1712.

3. Goswami D, Conway GS. Premature ovarian failure. *Hum Reprod Update*. 2005;11(4):391-410.

4. Eggan K, Jurga S, Gosden R, Min IM, Wagers AJ. Ovulated oocytes in adult mice derive from non-circulating germ cells. *Nature*. 2006;441(7097):1109-1114.

5. Zhai J, Yao G, Dong F, et al. In vitro activation of follicles and fresh tissue auto-transplantation in primary ovarian insufficiency patients. *J Clin Endocrinol Metab*. 2016;101(11):4405-4412.

6. Kawamura K, Cheng Y, Suzuki N, et al. Hippo signaling disruption and Akt stimulation of ovarian follicles for infertility treatment. *Proc Natl Acad Sci U S A*. 2013;110(43):17474-17479.

7. Jagarlamudi K, Reddy P, Adhikari D, Liu K. Genetically modified mouse models for premature ovarian failure (POF). *Mol Cellular Endocrinol*. 2010;315(1-2):1-10.

8. Danilovich N, Maysinger D, Sairam MR. Perspectives on reproductive senescence and biological aging: studies in genetically altered follitropin receptor knockout [FORKO] mice. *Exp Gerontol*. 2004;39(11-12):1669-1678.

9. Abbott BD, Schmid JE, Pitt JA, et al. Adverse reproductive outcomes in the transgenic Ah receptor-deficient mouse. *Toxicol Appl Pharmacol*. 1999;155(1):62-70.

10. Benedict JC, Miller KP, Lin TM, et al. Aryl hydrocarbon receptor regulates growth, but not atresia, of mouse preantral and antral follicles. *Biol Reprod*. 2003;68(5):1511-1517.

11. Lim J, Nakamura BN, Mohar I, Kavanagh TJ, Luderer U. Glutamate cysteine ligase modifier subunit (Gclm) null mice have increased ovarian oxidative stress and accelerated age-related ovarian failure. *Endocrinology*. 2015;156(9):3329-3343.

12. Kalich-Philosoph L, Roness H, Carmely A, et al. Cyclophosphamide triggers follicle activation and "burnout" AS101 prevents follicle loss and preserves fertility. *Sci Transl Med*. 2013;5(185): 185ra162.

13. Sonmezer M, Oktay K. Fertility preservation in young women undergoing breast cancer therapy. *Oncologist*. 2006;11(5): 422-434.

14. Zhang T, Yan D, Yang Y, et al. The comparison of animal models for premature ovarian failure established by several different source of inducers. *Regul Toxicol Pharmacol*. 2016;81:223-232.

15. Lee HJ, Selesniemi K, Niikura Y, et al. Bone marrow transplantation generates immature oocytes and rescues long-term fertility in a preclinical mouse model of chemotherapy-induced premature ovarian failure. *J Clin Oncol*. 2007;25(22):3198-3204.

16. Johnson J, Bagley J, Skaznik-Wikiel M, et al. Oocyte generation in adult mammalian ovaries by putative germ cells in bone marrow and peripheral blood. *Cell*. 2005;122(2):303-315.

17. Felicio LS, Nelson JF, Finch CE. Longitudinal studies of estrous cyclicity in aging C57BL/6 J mice: II. Cessation of cyclicity and the duration of persistent vaginal cornification. *Biol Reprod*. 1984;31(3):446-453.

18. Novella-Maestre E, Herraiz S, Rodriguez-Iglesias B, Diaz-Garcia C, Pellicer A. Short-Term PTEN inhibition improves in vitro activation of primordial follicles, preserves follicular viability, and restores AMH levels in cryopreserved ovarian tissue from cancer patients. *PLoS One*. 2015;10(5):e0127786.

19. Herraiz S, Buigues A, Diaz-Garcia C, et al. Fertility rescue and ovarian follicle growth promotion by bone marrow stem cell infusion. *Fertil Steril*. 2018;109(5):908-918.e2.

20. Herraiz S, Novella-Maestre E, Rodriguez B, et al. Improving ovarian tissue cryopreservation for oncologic patients: slow freezing versus vitrification, effect of different procedures and devices. *Fertil Steril*. 2014;101(3):775-784.

21. Johnson J, Canning J, Kaneko T, Pru JK, Tilly JL. Germline stem cells and follicular renewal in the postnatal mammalian ovary. *Nature*. 2004;428(6979):145-150.

22. Jiang Y, Zhao J, Qi HJ, et al. Accelerated ovarian aging in mice by treatment of busulfan and cyclophosphamide. *J Zhejiang Univ Sci B*. 2013;14(4):318-324.

23. Brydoy M, Fossa SD, Dahl O, Bjoro T. Gonadal dysfunction and fertility problems in cancer survivors. *Acta Oncol*. 2007;46(4):480-489.

24. Mayer LP, Dyer CA, Eastgard RL, Hoyer PB, Banka CL. Atherosclerotic lesion development in a novel ovary-intact mouse model of perimenopause. *Arterioscler Thromb Vasc Biol*. 2005;25(9):1910-1916.

25. Romero-Aleshire MJ, Diamond-Stanic MK, Hasty AH, Hoyer PB, Brooks HL. Loss of ovarian function in the VCD mouse-model of menopause leads to insulin resistance and a rapid progression into the metabolic syndrome. *Am J Physiol Regul Integr Comp Physiol*. 2009;297(3):R587-R592.

26. Van Kempen TA, Milner TA, Waters EM. Accelerated ovarian failure: a novel, chemically induced animal model of menopause. *Brain Res*. 2011;1379:176-187.

27. Ubaldi F, Vaiarelli A, D'Anna R, Rienzi L. Management of poor responders in IVF: is there anything new? *Biomed Res Int*. 2014;2014:352098.

28. Ataya K, Rao LV, Lawrence E, Kimmel R. Luteinizing hormone-releasing hormone agonist inhibits cyclophosphamide-induced ovarian follicular depletion in rhesus monkeys. *Biol Reprod*. 1995;52(2):365-372.

29. Meirow D, Lewis H, Nugent D, Epstein M. Subclinical depletion of primordial follicular reserve in mice treated with cyclophosphamide: clinical importance and proposed accurate investigative tool. *Hum Reprod*. 1999;14(7):1903-1907.

30. Grigg AP, McLachlan R, Zaja J, Szer J. Reproductive status in long-term bone marrow transplant survivors receiving busulfan-cyclophosphamide (120 mg/kg). *Bone Marrow Transplant*. 2000;26(10):1089-1095.

31. Hassan M, Andersson BS. Role of pharmacogenetics in busulfan/cyclophosphamide conditioning therapy prior to hematopoietic stem cell transplantation. *Pharmacogenomics*. 2013;14(1):75-87.

32. Generoso WM, Stout SK, Huff SW. Effects of alkylating chemicals on reproductive capacity of adult female mice. *Mutat Res*. 1971;13(2):172-184.

33. Batchvarov IS, Taylor RW, Bustamante-Marin X, et al. A grafted ovarian fragment rescues host fertility after chemotherapy. *Mol Hum Reprod*. 2016;22(12):842-851.

34. Nelson JF, Felicio LS, Randall PK, Sims C, Finch CE. A longitudinal study of estrous cyclicity in aging C57BL/6J mice: I. Cycle frequency, length and vaginal cytology. *Biol Reprod*. 1982;27(2):327-339.

35. Skaznik-Wikiel ME, McGuire MM, Sukhwani M, et al. Granulocyte colony-stimulating factor with or without stem cell factor extends time to premature ovarian insufficiency in female mice treated with alkylating chemotherapy. *Fertil Steril*. 2013;99(7):2045-2054 e2043.

36. Massin N, Gougeon A, Meduri G, et al. Significance of ovarian histology in the management of patients presenting a premature ovarian failure. *Hum Reprod*. 2004;19(11):2555-2560.

37. Massin N, Meduri G, Bachelot A, Misrahi M, Kuttenn F, Touraine P. Evaluation of different markers of the ovarian reserve in patients presenting with premature ovarian failure. *Mol Cell Endocrinol*. 2008;282(1-2):95-100.

38. Jiang Y, Zhao J, Qi H-J, et al. Accelerated ovarian aging in mice by treatment of busulfan and cyclophosphamide. *J Zhejiang Univ Sci B*. 2013;14(4):318-324.

39. Pedersen T, Peters H. Proposal for a classification of oocytes and follicles in the mouse ovary. *J Reprod Fertil*. 1968;17(3):555-557.

40. Edwards RG, Fowler RE, Gore-Langton RE, et al. Normal and abnormal follicular growth in mouse, rat and human ovaries. *J Reprod Fertil*. 1977;51(1):237-263.

41. Gougeon A. Regulation of ovarian follicular development in primates: facts and hypotheses. *Endocr Rev*. 1996;17(2):121-155.

42. McGee EA, Hsueh AJ. Initial and cyclic recruitment of ovarian follicles. *Endocr Rev*. 2000;21(2):200-214.

43. Richardson RB, Allan DS, Le Y. Greater organ involution in highly proliferative tissues associated with the early onset and acceleration of ageing in humans. *Exp Gerontol*. 2014;55:80-91.

44. Pan HA, Wu MH, Cheng YC, Wu LH, Chang FM. Quantification of ovarian stromal Doppler signals in poor responders undergoing in vitro fertilization with three-dimensional power Doppler ultrasonography. *Am J Obstet Gynecol*. 2004;190(2):338-344.

45. Pellicer A, Ballester MJ, Serrano MD, et al. Aetiological factors involved in the low response to gonadotrophins in infertile women with normal basal serum follicle stimulating hormone levels. *Hum Reprod*. 1994;9(5):806-811.

46. Battaglia C, Genazzani AD, Regnani G, Primavera MR, Petraglia F, Volpe A. Perifollicular Doppler flow and follicular fluid vascular endothelial growth factor concentrations in poor responders. *Fertil Steril*. 2000;74(4):809-812.

47. Weiner Z, Thaler I, Levron J, Lewit N, Itskovitz-Eldor J. Assessment of ovarian and uterine blood flow by transvaginal color Doppler in ovarian-stimulated women: correlation with the number of follicles and steroid hormone levels. *Fertil Steril*. 1993; 59(4):743-749.

48. Bassil S, Wyns C, Toussaint-Demylle D, Nisolle M, Gordts S, Donnez J. The relationship between ovarian vascularity and the duration of stimulation in in-vitro fertilization. *Hum Reprod*. 1997;12(6):1240-1245.

49. Lopez SG, Luderer U. Effects of cyclophosphamide and buthionine sulfoximine on ovarian glutathione and apoptosis. *Free Radic Biol Med*. 2004;36(11):1366-1377.

50. Plowchalk DR, Mattison DR. Reproductive toxicity of cyclophosphamide in the C57BL/6 N mouse: 1. Effects on ovarian structure and function. *Reprod Toxicol*. 1992;6(5):411-421.

51. Yuksel A, Bildik G, Senbabaoglu F, et al. The magnitude of gonadotoxicity of chemotherapy drugs on ovarian follicles and granulosa cells varies depending upon the category of the drugs and the type of granulosa cells. *Hum Reprod*. 2015;30(12): 2926-2935.

52. Herraiz S, Romeu M, Buigues A, et al. Autologous stem cell ovarian transplantation to increase reproductive potential in patients who are poor responders. *Fertil Steril*. 2018;110(3): 496-505.